Supplementary Information

Supplementary Note 1. Homology model construction for *E. coli* DNA gyrase and topoisomerase IV. As the X-ray crystal structures of the protein targets of *E. coli* are not available, we have built homology models of DNA gyrase and topoisomerase IV based on structural templates from *Staphylococcus aureus* and *K. pneumoniae*, respectively (see Materials and Methods). To construct homology models of *E. coli* DNA gyrase and topoisomerase IV, homologous bacterial protein sequences were downloaded from UniProt (https://www.uniprot.org/) (see also Methods). Sequence alignments were carried out using the Schrödinger Program Suite(1) with BLOSUM62 substitution matrix, with -10.0 as gap opening and -1.0 as gap extension penalty. **Supplementary Table S1** lists sequence identities and homologies of target-template sequence pairs used in our homology model construction.

Target-template pairs	Identity (%)	Homology (%)
GyrA P0AES4-P20831	**50**	**69**
GyrB P0AES6-P0A0K8	**44**	**56**
ParC P0AFI2-R4YE07	**95**	**97**
ParE P20083-R4YHS8	**94**	**97**

Supplementary Table S1. Sequence identity and homology of target sequences GyrA(P0AES4), GyrB(P0AES6) chains of DNA gyrase and ParC(P0AFI2), ParE(P20083) chains of topoisomerase IV of *E. coli* K-12, compared to their template structures from *Staphylococcus aureus* (GyrA(P20831), GyrB(P0A0K8)) and *K. pneumoniae* (ParC(R4YE07), ParE(R4YHS8)), respectively.

Supplementary Note 2. Two alternative binding poses of gepotidacin at *E. coli* DNA gyrase and topoisomerase IV. The binding sites for gepotidacin at both DNA gyrase and topoisomerase IV are located at the interface of the GyrA and ParC subunits, respectively (Figure 1). These two subunits together form the mainly hydrophobic binding pocket of gepotidacin. Based on our model, only a single strong, non-hydrophobic interaction appears between gepotidacin and the target proteins, namely a salt-bridge formed by gepotidacin with D82 in the GyrA subunit of DNA gyrase and D79 in the ParC subunit of topoisomerase IV. However, due to the symmetry of this binding cavity at both subunits (GyrA and ParC), the reconstructed binding modes contained two alternative binding poses (see Supplementary Figure S1). Both of these binding poses show an approximately 2-fold rotational symmetry in their orientation, and this way the triazaacenaphthylene ring intercalates DNA in a 180 degree-rotated orientation compared to each other. The protonated secondary nitrogen of gepotidacin also changes its dominant interaction with D82 of GyrA and D79 of ParC from one chain to the other, respectively, on both targets. The pyranopiridine ring is also turned around, but it occupies the same hydrophobic pocket. Because of the symmetrical arrangement of the two binding modes, only one of them was used in our further analyses. As a confirmation for these binding modes, the molecular dynamics simulations also proved that the initial binding positions of gepotidacin in wild-type proteins are stable: the average root mean square deviations (RMSD) of heavy atom coordinates of gepotidacin during the second half of the simulation from the initial pose was 1.24±0.27Å for the wild-type DNA gyrase, and 1.10±0.14Å for the wild-type topoisomerase IV. This means that the initial positions were somewhat changed during the simulation, but the systems could reach equilibrium positions close to the initial one with small average fluctuations.

Supplementary Figure S1. Intermolecular interactions between gepotidacin and its binding-site forming amino acids at DNA gyrase (A) and topoisomerase IV (B). Green lines indicate drug-target interactions with DNA nucleobases; purple line indicates salt bridge between gepotidacin and GyrA D82 (**A**), and ParC D79 residues (**B**) respectively. Results are based on 100 nanosecond long molecular dynamics simulations of gepotidacin-bound *E. coli* DNA gyrase and topoisomerase IV complexes. Figure displays binding-site forming amino acids and DNA nucleobases (in grey) that are closer than 4Å to gepotidacin at DNA gyrase and topoisomerase IV. D82N (GyrA) and D79N (ParC) mutations leave this interaction pattern unchanged but increase the binding free energies in both cases as it is indicated by the $\Delta\Delta G_B$ values (obtained from MM-GBSA calculations) in panel A and B, respectively.

A

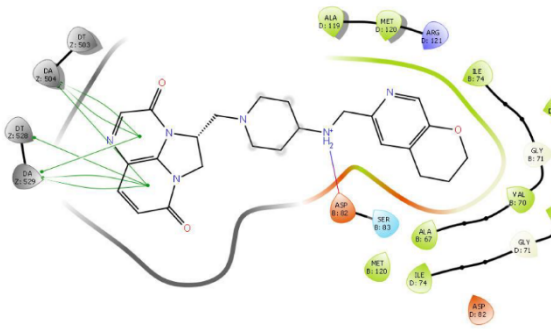

$\Delta\Delta G_{D82 \rightarrow N82}$ = 5.44±2.92 kcal/mol

B

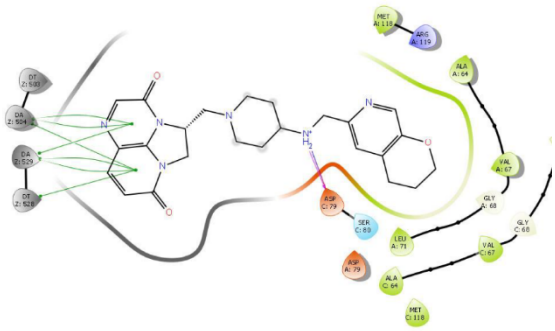

$\Delta\Delta G_{D79 \rightarrow N79}$ = 4.43±1.71 kcal/mol

Supplementary Figure S2. Two alternative binding poses of gepotidacin in the homology model of *E. coli* K-12 DNA gyrase. Gepotidacin appears in ball-and-stick representation, the DNA chain is shown as thin sticks, the two GyrA chains (B and D) are in ribbon representation, and D82 residues of GyrA are represented as balls, while S83 and R119 appear as sticks.

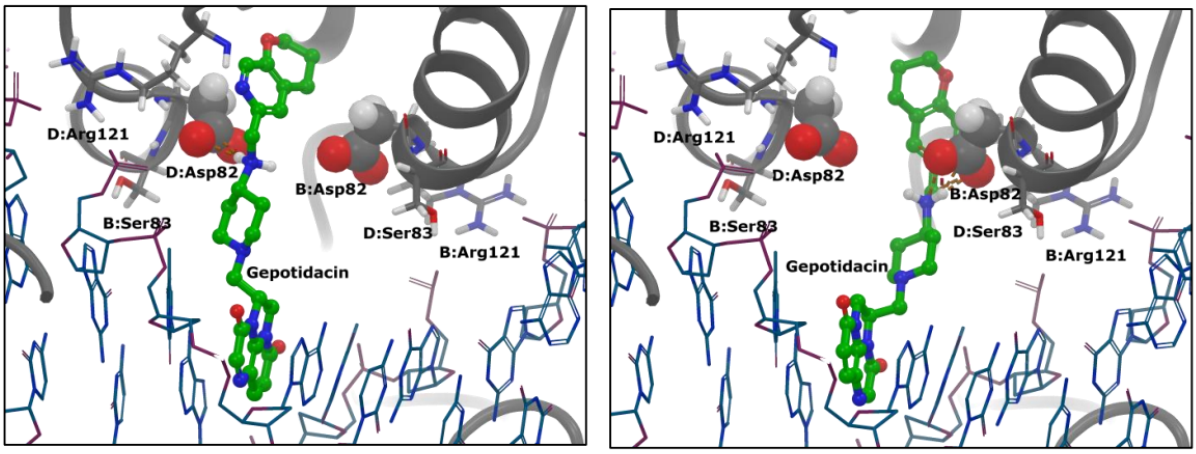

Supplementary Table S2. The studied mutations are prevalent in bacterial populations never treated with gepotidacin. Literature data referring to mutations associated with reduced susceptibility to gepotidacin and their prevalence in human clinical pathogens. Amino acid positions are marked according to their corresponding residue in *Escherichia coli* K-12 MG1655. N.a denotes observed mutation (prevalence = single case) with no available prevalence, *mut* denotes any mutation at a given position. Screening of the publicly available nucleotide archive of the National Center for Biotechnology Information (NCBI) shows an abundance of the aforementioned mutations in other sequencing data as well, in multiple human-associated bacterial species.

Species	Detected mutations	Prevalence (%)/ Strain number	Source
Salmonella enterica	GyrA D82N	2.9–10%	Eaves, D. J. et al. 2004.(2)
Neisseria gonorrhoeae	ParC D79N	54%	Su, X. et al. 2001.(3)
Neisseria gonorrhoeae	ParC D79N	16.90%	Jacobsson, S. et. al. 2018.(4) + Homology search
Salmonella enterica serovar Typhimurium	GyrA D82*mut*	100%	Thong, K. L. et al. 2015.(5)
Mycoplasma genitalium	ParC D79N	1.60%	Hamasuna, R. et al. 2018.(6)
Salmonella enterica serovar Typhimurium	GyrA D82N	n.a.	Randall, L. P. et. al. 2005.(7)
Salmonella enterica serovar Typhi	GyrA D82N	n.a.	García-Fernández, A. et al. 2015.(8)
Bifidobacterium breve	GyrA D82N	8	Homology search from NCBI database
Mycoplasma bovis	GyrA D82N	2	Homology search from NCBI database
Clostridium difficile	GyrA D82N	2	Homology search from NCBI database
Cutibacterium acnes	GyrA D82N	1	Homology search from NCBI database
Salmonella enterica serovar Infantis	GyrA D82N	1	Homology search from NCBI database
Mycobacterium malmoense	GyrA D82N	1	Homology search from NCBI database
Citrobacter sp.	ParC D79N	1	Homology search from NCBI database
Streptococcus pneumoniae	ParC D79N	1	Homology search from NCBI database

Neisseria gonorrhoeae	ParC D79N	13	Homology search from NCBI database

Supplementary Figure S3. tBLASTn analysis identified genotypes associated with reduced susceptibility to gepotidacin in the nucleotide archive of the National Center for Biotechnology Information (NCBI). See Supplementary File 1 for taxon identifiers, GeneBank IDs, and analyzed protein sequences.

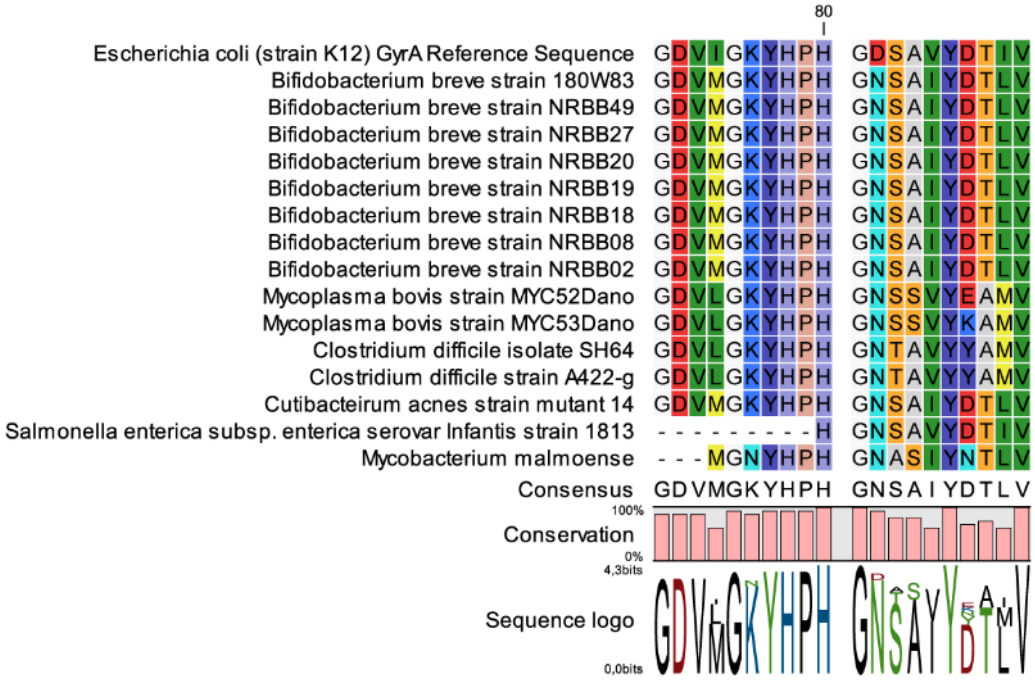

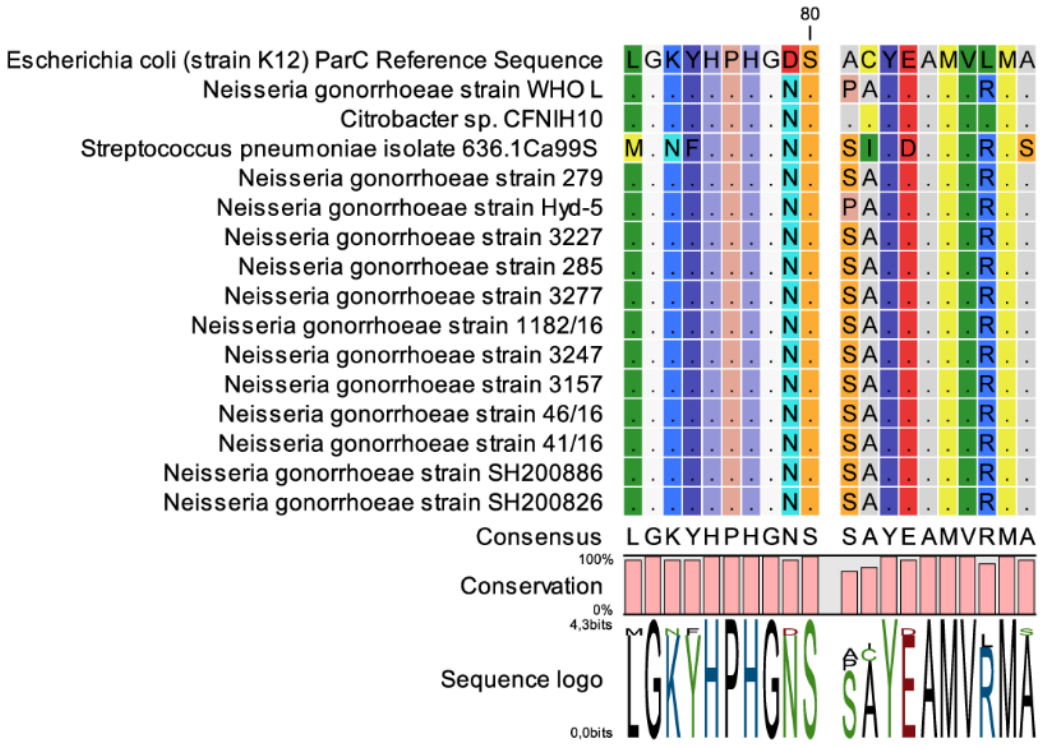

Supplementary Table S3. Whole genome sequence analysis of laboratory-adapted, ciprofloxacin-resistance conferring variants of *Klebsiella pneumoniae* ATCC 10031 and *Escherichia coli* K-12 MG1655.

Linage	Genomic position	Type	Reference	Allele	Gene	Amino acid change
Klebsiella pneumoniae ATCC 10031						
E2	1177644	SNV	T	G	gyrA	Y548D
	3454728	DEL	CAT	C	bm3R1	Frameshift
	5009863	SNV	T	C	rpoB	D675G
E4	811416	SNV	T	G	cusS	S260A
	1177644	SNV	T	G	gyrA	Y548D
	3454728	DEL	CAT	C	bm3R1	Frameshift
	5009863	SNV	T	C	rpoB	D675G
E6	811416	SNV	T	G	cusS	S260A
	811421	SNV	C	T	cusS	N261N
	811427	SNV	C	T	cusS	S263S
	1176261	SNV	G	T	gyrA	D87Y
	1177644	SNV	T	G	gyrA	Y548D
	3454728	DEL	CAT	C	bm3R1	Frameshift
	5009863	SNV	T	C	rpoB	D675G
Escherichia coli K-12 MG1655						
E8	485845	INS	G	GTA	acrR	Frameshift
	2339176	INS	T	TCAC	gyrA	Frameshift
	3878726	SNV	T	G	gyrB	Q465P
	4114421	SNV	C	A	fpr	A18S
	4182842	DEL	TCGGCCCAGG	T	rpoB	Frameshift
	4277526	SNV	C	A	soxR	R20S
	485845	INS	G	GTA	acrR	Frameshift
E10	485934	SNV	G	T	acrR	L58F
	924967	INS	A	AG	clpA	Frameshift
	1342333	SNV	T	A	pyrF	L138Q
	1619348	SNV	C	T	marR	R77C
	1910623	SNV	C	T	yebQ	F116F
	2339162	SNV	C	T	gyrA	D87N
	2631101	SNV	C	A	guaA	D479Y
	3377148	INS	A	AACAGG	sspA	Frameshift
	3554605	DEL	ACTGG	A	malT	Frameshift
	4184974	SNV	C	A	rpoB	H1244N
	4634724	INS	A	ACCT	rob	Frameshift

Supplementary Table S4. Sequence analysis of DIvERGE-generated mutants of *Klebsiella pneumoniae* ATCC 10031 conferring reduced susceptibility to gepotidacin. Clones were selected at the peak plasma concentration of gepotidacin (9 µg/ml).

Library	Clone ID	Mutation at GyrA	Mutation at ParC
DIvERGE mutagenesis of *K. pneumoniae* GyrA and ParC	#1	D82N	D79N
	#2	D82N	D79N
	#3	D82N	D79N
	#4	D82N	D79N
	#5	D82N	D79N
	#6	D82N	D79N
	#7	D82N	D79N
	#8	D82N	D79N
	#9	D82N	D79N
	#10	D82N	D79N
Saturation mutagenesis of *K. pneumoniae* GyrA D82 and ParC D79	#1	D82N	D79N
	#2	D82N	D79N
	#3	D82N	D79N
	#4	D82N	D79N
	#5	D82N	D79N
	#6	D82N	D79N
	#7	D82N	D79N
	#8	D82N	D79N
	#9	D82N	D79N
	#10	D82N	D79N

Supplementary Table S5. Gepotidacin and ciprofloxacin minimal inhibitory concentration of single-step mutations and their combination in *Escherichia coli* K-12 MG1655 and *Klebsiella pneumoniae* ATCC 10031. Growth inhibition was determined by optical density (OD_{600}) measurements of the bacterial culture after 18 h incubation in the presence of the corresponding drug concentration, according to the EUCAST guidelines(9). Results presented here as the mean of 9 independent replicates respectively.

Mutant genotype	Ciprofloxacin MIC (µg/ml)	Gepotidacin MIC (µg/ml)
E. coli K-12 MG1655 wild-type	0.016	0.25
E. coli K-12 MG1655 GyrA S83L	0.063	0.125
E. coli K-12 MG1655 GyrA S83L, D87N	0.25	0.25
E. coli K-12 MG1655 GyrA S83L, D87N; ParC S80I	20	0.125
E. coli K-12 MG1655 GyrA S83L, D87Y; ParC S80I, E84G	32	0.125
K. pneumoniae ssp. pneumoniae ATCC 10031 wild-type	0.004	0.063
K. pneumoniae ssp. pneumoniae ATCC 10031 GyrA S83F	0.08	0.5
K. pneumoniae ssp. pneumoniae ATCC 10031 GyrA S83F, D87G	0.125	0.25
K. pneumoniae ssp. pneumoniae ATCC 10031 GyrA S83F, D87G; ParC S80I	2	0.063
K. pneumoniae ssp. pneumoniae ATCC 10031 GyrA S83F, D87G; ParC S80I, E84G	4	0.31

References

1. 2017. Small-Molecule Drug Discovery Suite 2017-4. Schrödinger, LLC, New York, NY.

2. Eaves DJ, Randall L, Gray DT, Buckley A, Woodward MJ, White AP, Piddock LJV. 2004. Prevalence of Mutations within the Quinolone Resistance-Determining Region of gyrA, gyrB, parC, and parE and Association with Antibiotic Resistance in Quinolone-Resistant Salmonella enterica. Antimicrob Agents Chemother 48:4012–4015.

3. Su X, Lind I. 2001. Molecular Basis of High-Level Ciprofloxacin Resistance in Neisseria gonorrhoeae Strains Isolated in Denmark from 1995 to 1998. Antimicrob Agents Chemother 45:117–123.

4. Jacobsson S, Golparian D, Scangarella-Oman N, Unemo M. In vitro activity of the novel triazaacenaphthylene gepotidacin (GSK2140944) against MDR Neisseria gonorrhoeae. J Antimicrob Chemother. 2018, 73.8: 2072-2077.

5. Thong KL, Ngoi ST, Chai LC, Teh CSJ. 2015. Quinolone Resistance Mechanisms Among Salmonella enterica in Malaysia. Microb Drug Resist 22:259–272.

6. Hamasuna, R., Le, P. T., Kutsuna, S., Furubayashi, K., Matsumoto, M., Ohmagari, N., ... & Jensen, J. S. (2018). Mutations in ParC and GyrA of moxifloxacin-resistant and susceptible Mycoplasma genitalium strains. PloS one, 13(6), e0198355.

7. Randall LP, Coldham NG, Woodward MJ. 2005. Detection of mutations in Salmonella entericagyrA, gyrB, parC and parE genes by denaturing high performance liquid chromatography (DHPLC) using standard HPLC instrumentation. J Antimicrob Chemother 56:619–623.

8. García-Fernández A, Gallina S, Owczarek S, Dionisi AM, Benedetti I, Decastelli L, Luzzi I. 2015. Emergence of Ciprofloxacin-Resistant Salmonella enterica Serovar Typhi in Italy. PLOS ONE 10:e0132065.

9. ISO 20776-1:2006 - Clinical laboratory testing and in vitro diagnostic test systems -- Susceptibility testing of infectious agents and evaluation of performance of antimicrobial susceptibility test devices -- Part 1: Reference method for testing the in vitro activity of

antimicrobial agents against rapidly growing aerobic bacteria involved in infectious diseases.

ISO.